NIH Public Access
Author Manuscript
J Invest Dermatol. Author manuscript; available in PMC 2011 September 8.

Published in final edited form as:
J Invest Dermatol. 2009 February ; 129(2): 348–354. doi:10.1038/jid.2008.212.

Pseudoxanthoma Elasticum is a Metabolic Disease

Qiujie Jiang[1], **Masayuki Endoh**[2], **Florian Dibra**[1], **Krystle Wang**[1], and **Jouni Uitto**[1]
[1]Departments of Dermatology and Cutaneous Biology, Thomas Jefferson University, Philadelphia, PA USA

[2]The Children's Hospital of Philadelphia, Philadelphia, PA

Abstract

Pseudoxanthoma elasticum (PXE) is a pleiotropic multisystem disorder affecting skin, eyes, and the cardiovascular system with progressive pathological mineralization. It is caused by mutations in the *ABCC6* gene expressed primarily in the liver and kidneys, and at very low levels, if at all, in tissues affected by PXE. A question has arisen regarding the pathomechanism of PXE, particularly the "metabolic" versus the "PXE cell" hypotheses. We examined a murine PXE model (*Abcc6*$^{-/-}$) by transplanting muzzle skin from knock-out (KO) and wild-type (WT) mice onto the back of WT and KO mice using mineralization of the connective tissue capsule surrounding the vibrissae as an early phenotypic biomarker. Grafting of WT mouse muzzle skin onto the back of KO mice resulted in mineralization of vibrissae, while grafting KO mouse muzzle skin onto the WT mice did not. Thus, these findings implicate circulatory factors as a critical component of the mineralization process. This mouse grafting model supports the notion that PXE is a systemic metabolic disorder with secondary mineralization of connective tissues and that the mineralization process can be countered or even reversed by changes in the homeostatic milieu.

INTRODUCTION

Pseudoxanthoma elasticum (PXE; OMIM 264800) is a multi-system disorder characterized by progressive mineralization of connective tissues, primarily affecting the elastic structures in the skin, Bruch's membrane of the retina, and the mid-layers of the arterial blood vessels (Li *et al*, 2008; Neldner and Struk, 2002; Ringpfeil *et al.*, 2001). PXE is caused by mutations in the *ABCC6* gene which encodes ABCC6, a protein belonging to the family of ATP-binding cassette proteins (Pfendner *et al.*, 2007, 2008). *ABCC6* is expressed primarily in the basolateral surface of the hepatocytes, to a lesser extent in the proximal tubules of the kidneys, and at a very low level, if at all, in resident cells, such as fibroblasts and smooth muscle cells, in tissues affected by PXE (Belinsky and Kruh, 1999; Matsuzaki *et al.*, 2005; Scheffer *et al.*, 2002). On the basis of structural homology with other ABCC transporters, particularly ABCC1, the prototype of C family of these proteins, ABCC6 has been suggested to serve as an efflux transporter molecule, and *in vitro* experiments have suggested that glutathione conjugated anionic molecules can serve as transport substrates (Belinsky *et al.*, 2002; Iliás *et al.*, 2002). However, the precise function of ABCC6 and its physiologic substrates *in vivo* remain unknown, and the pathomechanistic details leading from *ABCC6* mutations to aberrant mineralization in peripheral tissues remain to be explored. Furthermore, PXE shows considerable phenotypic variability, and a number of

Address for Correspondence: Jouni Uitto, M.D., Ph.D., Department of Dermatology and Cutaneous Biology, Jefferson Medical College, 233 S. 10th Street, Suite 450 BLSB, Philadelphia, PA 19107, USA, Tel: (215) 503-5785, Fax: (215) 503-5788, Jouni.Uitto@jefferson.edu.

Conflict of Interest
The authors state no conflict of interest.

NIH-PA Author Manuscript
NIH-PA Author Manuscript
NIH-PA Author Manuscript

NIH-PA Author Manuscript

NIH-PA Author Manuscript

NIH-PA Author Manuscript

modifying factors, both genetic and environmental, have been suggested to play a role (Hendig *et al.*, 2007, 2008; Neldner and Struk, 2002; Zarbock *et al.*, 2007).

Two general mechanisms have been proposed to explain the consequences of the *ABCC6* mutations in PXE as manifested by mineralization of the elastic structures and collagen fibers in the skin, the eyes, and the cardiovascular system. “The metabolic hypothesis” postulates that in the absence of functional ABCC6 activity, primarily in the liver, there are changes in the levels of circulating factor(s) that are physiologically required to prevent unwanted mineralization (Jiang *et al.*, 2007; Uitto *et al.*, 2001). In support of the metabolic hypothesis are the clinical observations and our PXE mouse model studies (see below) indicating that PXE is a late-onset, slowly progressing condition. In further support of this hypothesis are demonstrations that serum from PXE patients and mice lack the capacity to prevent calcium/phosphate precipitation in an *in vitro* assay utilizing smooth muscle cell cultures (Jiang *et al.*, 2007). In addition, serum from patients with PXE has been shown to modulate the elastin biosynthetic profile in cultured dermal fibroblasts, further implicating circulatory factors in the disease process (LeSaux *et al.*, 2006). On the other hand, “the PXE cell hypothesis” postulates that the lack of ABCC6 expression in the resident cells alters their biosynthetic capacity and biological profile (Quaglino *et al.*, 2000, 2005). Specifically, cultured fibroblasts derived from the skin of patients with PXE demonstrate increased extracellular matrix expression, enhanced degradative potential, and altered cell-cell and cell-matrix interactions, associated with changes in their proliferative capacity. In support of this postulate are also the histopathological and ultrastructural observations demonstrating that the elastic structures that become mineralized in the skin of patients with PXE are not normal elastic fibers but appear to have a changed composition. Nevertheless, both hypotheses lack strong experimental evidences and remain to be confirmed.

We have developed an *Abcc6*$^{-/-}$ knock-out (KO) mouse by targeted ablation of the corresponding gene (Klement *et al.*, 2005). These mice show normal natal and postnatal development and are morphologically and histologically indistinguishable from their wild-type (WT) counterparts during the early postnatal period. However, at ~5 weeks of age, progressive mineralization affecting soft connective tissues ensues in homozygous *Abcc6*$^{-/-}$ mice, but not in their heterozygous litter mates or WT counterparts. Electron microscopy revealed that the mineralization process affects both elastic structures and collagen fibers (Klement *et al*, 2005). Specifically, these mice demonstrate extensive mineralization of connective tissues in the skin, the eyes, and the cardiovascular system, *i.e.*, tissues affected in PXE. Thus, these mice recapitulate the genetic, histopathologic and ultrastructural features of human PXE. An intriguing feature of these mice is that the first site of mineralization is the connective tissue capsule surrounding the bulb of vibrissae, which then serves as an early biomarker of the PXE mineralization process in these mice (Jiang *et al.*, 2007; Klement *et al.*, 2005).

In this study, we have addressed the “metabolic hypothesis” of PXE utilizing the *Abcc6*$^{-/-}$ mice as a model system. Specifically, we have grafted muzzle skin containing the vibrissae from WT and KO mice onto the back of KO and WT mice. The degree of mineralization was evaluated by histopathology, including special stains for calcium and phosphate, followed by computerized morphometric analysis.

RESULTS

Experimental designs

Two experimental designs were utilized: one of them was used to examine potential *prevention* of ectopic mineralization, while the second one was aimed at examining the potential of *reversal* of the mineralization. In the *prevention study*, muzzle skin from WT or

NIH-PA Author Manuscript

NIH-PA Author Manuscript

NIH-PA Author Manuscript

KO mice at 4 weeks of age (before development of mineral deposits) was transplanted onto the back of both KO and WT mice; in the *reversal study*, muzzle skin from KO mice at 12 weeks (after development of mineralization) was transplanted onto WT or KO mice.

Assessment of the graft viability

Both designs utilized skin grafts from the muzzle skin either from the WT or *Abcc6*$^{-/-}$ KO mice, which were transplanted onto the back of either WT or KO mice. The overall success rate and persistence of the grafts was 83%. At the time points indicated below, the grafts together with surrounding recipient skin, were removed and examined by H&E stain to assess the presence and viability of the graft. Specifically, the presence of cross sections of vibrissae, as shown in Figure 1b, was characteristic of the donor muzzle skin, while the adjacent back skin of the recipient did not have these structures, indicating the persistence of the graft. The origin of the graft was also verified by genomic PCR. Specifically, the grafts which originated from the KO mice demonstrated the presence of a 320 bp PCR product representing the *Abcc6*$^{-/-}$ allele, while the grafts originating from the WT mice clearly demonstrated the presence of 430 bp wild-type allele of *Abcc6* (Figure 1c, groups 1 and 2, respectively).

Progression of mineralization in *Abcc6*$^{-/-}$ mice

In order to establish the reference points of mineralization for the grafting studies, the progressive nature of ectopic mineralization of the connective tissue capsule of vibrissae was examined in *Abcc6*$^{+/+}$ and *Abcc6*$^{-/-}$ mice (Figure 2). As reported previously (Klement *et al.*, 2005), no mineralization can be noted in *Abcc6*$^{+/+}$ mice even up to two years of age, and this was confirmed in our study. Specifically, there was no evidence of mineralization in *Abcc6*$^{+/+}$ mice at 24 weeks when the capsules were stained either with H&E, Alizarin Red or with von Kossa stain (Figure 2a,e, and i). In *Abcc6*$^{-/-}$ mice, no evidence of mineralization was noted at 4 weeks, but foci of mineralization were detected at 12 weeks of age and the mineralization progressively increased in the subsequent 12 weeks (Figure 2).

Evidence for the metabolic nature of PXE

In the first set of experiments (*prevention*) addressing the metabolic hypothesis of PXE, muzzle skin grafts were placed onto the back of mice at 4 weeks of age, a time point that did not show any degree of mineralization in the *Abcc6*$^{-/-}$ mice. Three different experimental groups were studied. Group 1: Muzzle skin from *Abcc6*$^{+/+}$ mouse (donor) was grafted onto the back of gender- and age-matched *Abcc6*$^{-/-}$ mouse (recipient). Group 2: The same set-up as in Group 1, except that the *Abcc6*$^{-/-}$ mouse was the donor and the *Abcc6*$^{+/+}$ mouse was the recipient. Group 3: both donor and recipient were *Abcc6*$^{+/+}$ mice. The grafts were then examined at two months subsequent to the placement of the graft. When WT mouse muzzle skin was transplanted onto the back of a recipient KO mouse, evidence of mineralization could be noted in the connective tissue capsule surrounding the vibrissae in each mouse (Figure 3a–c, arrows), although not every vibrissa showed mineralization, the total percent of mineralized vibrissae being 28.6% of all examined (Table 1). In contrast, placement of KO mouse muzzle skin onto the back of WT mice did not reveal any evidence of mineralization at 2 months post-operatively (Figure 3d–f). Finally, placement of WT mouse muzzle skin onto the back of another WT mouse did not result in mineralization (Figure 3g–i), indicating that the mineralization noted in the KO mouse is not due to surgical manipulation. The results illustrated in Fig. 3 were based on survey of 56, 42 and 12 vibrissae in Groups 1, 2 and 3, respectively. As shown in Table 1, 16 out of 56 vibrissae grafted from the muzzle skin of *Abcc6*$^{+/+}$ mice onto the back of *Abcc6*$^{-/-}$ mice (Group 1) developed characteristic mineralization, while no mineralization was observed in any of the 42 and 12 vibrissae examined in Groups 2 and 3, respectively. The connective tissue mineralization could also be visualized by transmission electron microscopy of the graft

NIH-PA Author Manuscript

NIH-PA Author Manuscript

NIH-PA Author Manuscript

from WT mice muzzle skin placed on the back of the KO mice. Examination of different areas of tissue revealed that both collagen fibers and elastic tissue depicted characteristic electron dense mineral deposits (Figure 3j,k), similar to that seen in humans with PXE (Neldner and Struk, 2002; Ringpfeil *et al.*, 2001).

The above *prevention* studies were performed utilizing 8 and 7 individual pairs of mice in Group 1 and Group 2, respectively. The pairs represented the same litter, and the mice were originally developed on mixed C57/J129 background and had been cross-bred towards C57 genetic homogeneity for six generations. Nevertheless, 2 and 1 mice in Groups 1 and 2, respectively, showed histologic evidence of inflammation, suggesting minor immune incompatibility. Consequently, similar experiments were performed with immune deficient *Rag 1* mice *(Abcc6*$^{+/+}$*)* (Mombaerts *et al.*, 1992) as the recipients of muzzle skin grafts from *Abcc6*$^{-/-}$ mice (n=3). Examination of these grafts did not reveal any evidence of immune reaction and there was no mineralization, validating the original observations in the KO→ WT group of mice (Group 2).

Collectively, these data clearly imply that PXE does not result from a localized defect based on abnormalities in the resident cells in affected tissues, but rather from a change of metabolite(s) in serum that would physiologically prevent the mineralization process in ectopic tissue sites.

Potential for reversal of mineralization in PXE

In general, mineralization develops in several stages: amorphous calcium phosphate is deposited at the early stages of the process and then gradually transforms into the less soluble crystalline apatite-like compounds (Carson, 1997). Therefore, in the second set of experiments, aimed at evaluation of the potential for *reversal* of the mineralization, muzzle skin from *Abcc6*$^{-/-}$ mice at 12 weeks, *i.e.*, after the development of mineralization had commenced (see Figure 2), was transplanted onto the back of *Abcc6*$^{+/+}$ or *Abcc6*$^{-/-}$ mice. As a control, the muzzle skin from *Abcc6*$^{-/-}$ mice at 3 months of age was also examined. Quantitation of mineralization of the connective tissue capsule surrounding the vibrissae revealed clear evidence of mineralization in KO mice (n=11) at 3 months of age, *i.e.*, at the time the grafting procedure was initiated. The difference in the degree of mineralization among the three groups was significant (p=0.0154; Kruskal-Wallis Test) (Table 2). Examination of the grafts originating from the *Abcc6*$^{-/-}$ mice and placed on the back of WT mice showed significantly less mineralization than those grafts placed on the back of KO mice ($p<0.05$; Dunn's Multiple Comparison Test). In contrast, the grafts originating from KO mice and placed on the back of *Abcc6*$^{-/-}$ indicated close to a 2.5-fold increase in the degree of mineralization in the subsequent three months after grafting, as compared to the three-month old mice. However, due to individual variability, this difference did not reach statistical significance ($p>0.05$) (Table 2). The mean degree of mineralization in the KO→ WT group was about 60% less than noted in the muzzle skin of KO mice at 3 months of age, but this difference was not statistically significant ($p> 0.05$) (Table 2).

Conclusions and clinical implications

In this study, we have utilized mouse skin transplantation using a mouse PXE model (*Abcc6*$^{-/-}$). After grafting, vascular capillaries in the graft regress while new vascular in growth occurs from the wound bed to replace the regressing vessels (Capla *et al.*, 2006; Matsuo *et al.*, 2007). The survival of skin grafts is, therefore, dependent on the reestablishment of an adequate blood circulation ingrown from the recipient animal. New established capillaries were also observed in our study (data not shown). Thus, all survived grafts were supplied by the blood of the recipient mice. If PXE is a metabolic disorder, one would expect that the *Abcc6*$^{-/-}$ mouse skin graft would not develop mineralization on the

NIH-PA Author Manuscript

NIH-PA Author Manuscript

NIH-PA Author Manuscript

Abcc6$^{+/+}$ mouse, but the skin from WT mouse would be mineralized after grafting onto *Abcc6*$^{-/-}$ mouse. This was indeed observed in our experiments, suggesting that circulating factor(s) in the recipient's blood play a critical role in determining the degree of mineralization of the graft, irrespective of graft genotype. It is important to note that our studies do not shed light on the chemical characteristics or the mechanistic details of action of the circulatory factors playing a role in the pathologic mineralization in PXE. Previously, a number of serum proteins, including matrix gla protien, fetuin-A and ankylosis protein, have been shown to prevent unwanted mineralization under physiologic conditions of mineral homeostasis (see Jiang *et al*, 2007). More recently, low-molecular-weight compounds, such as vitamin K derivatives, alone or conjugated with glutathione, have emerged as potential effector molecules (Li *et al*, 2008). Finally, the mechanistic details of the mineralization process, whether humoral or cellular, are not clear. A possibility potentially bridging the observations in support of "metabolic" versus "PXE cell" hypothesis is that the circulatory factors, or the lack thereof, influence the metabolic profile of target cells, such as fibroblasts in the peripheral connective tissues, thus eliciting the processes leading to ectopic mineralization (Gheduzzi *et al*, 2007).

Collectively, this mouse grafting model supports the notion that PXE is a systemic metabolic disease, and that the pathologic deposition of minerals onto the affected tissues can be prevented and even reversed under physiologic homeostatic conditions. These findings may have implications for future treatment of this, currently intractable, disorder. More specifically, identification of the critical factor(s) in circulation influencing the pathologic mineralization of peripheral connective tissues could provide novel strategies to counteract mineral deposition with subsequent improvement in the clinical manifestations of PXE (Li *et al.*, 2008).

MATERIALS AND METHODS

Mice and study design

The PXE mouse model, *Abcc6*$^{-/-}$ KO, mouse was developed by targeted inactivation of the *Abcc6* gene (Klement *et al.*, 2005). The mice were maintained under pathogen-free conditions and were handled in accordance with the guidelines for animal experiments by the Institutional Animal Care and Use Committee of Thomas Jefferson University. The experiments were initiated when the mice were 4 weeks or 12 weeks of age. The mice were originally developed on C57/J129 genetic background and cross-bred towards C57 genetic homogeneity for six generations. In each experiment, *Abcc6*$^{+/+}$ and *Abcc6*$^{-/-}$ mice from the same litter were used. In some experiments, *Rag1* (*Abcc6*$^{+/+}$) mice (Jackson Labs) were used as recipients.

Transplant surgical techniques

Grafting surgery was performed in a laminar-flowhood using sterile procedures. General anesthesia was accomplished by isoflurane delivered by a precision vaporizer. The recipient mouse back skin was cleaned with sterile saline and shaved. The donor mouse muzzle skin (0.5–1.0 cm in diameter) was dissected at the level of the subcutis and then rinsed in calcium-and magnesium-free PBS (pH 7.4) containing antibiotics. The skin was grafted, within0.5 h of harvest, to a wound bed of similar size that was prepared by removing recipient mouse skin from the side of the dorsal region (Figure 1a). Xeroform, a non-adherent petrolatum dressing, was applied on the top of the graft, covered by an adhesive dressing and left in place for 1 week.

NIH-PA Author Manuscript

NIH-PA Author Manuscript

NIH-PA Author Manuscript

Histopathology and transmission electron microscopy

The graft or muzzle skin was fixed in 10% phosphate-buffered formalin, embedded in paraffin, sectioned (5μm), and stained with hematoxylin-eosin (H&E), Alizarin Red and von Kossa using standard methods for histopathological analyses. For transmission electron microscopy (TEM), muzzle skin samples were prepared using standard protocols. Sections were examined and photographed at 80 kV using a Tecnai 12 transmission electron microscope equipped with a Gatan US1000 2K Ultrascan digital camera.

Computerized morphometric quantitation of graft mineralization by histopathology

Computerized morphometric analysis of H&E stained sections of graft was performed as described elsewhere (LaRusso *et al.*, 2007; Li *et al.*, 2007). Briefly, seven sections from each graft were examined with a Nikon model TE2000 microscope equipped with an AutoQuant Imaging system (Watervliet, New York, N.Y.). The number of vibrissae, both those with evidence of mineralization and those without, were determined in 4–20 systemically selected fields, so that the images capture every visible vibrissae in each section. The degree of mineralization was expressed as pixels (arbitrary units) per graft and calculated as the percentage of area of mineralization per total area of vibrissae.

Genotyping

The genotype of the grafts was determined by genomic PCR. DNA was isolated from a full-thickness graft in the diameter of 2 mm. The PCR was performed with three primers designed for amplification of the KO (320-bp), WT (430-bp), or both alleles in the same reaction, as described previously (Klement *et al.*, 2005).

Statistical analysis

Results are given as mean ± SEM and as median plus range. The data were analyzed first by Kruskal-Wallis Test using Graph Pad Prism Software (San Diego, CA) followed by Dunn's Multiple Comparison Test for the pairwise analyses. Differences were considered significant if $p<0.05$.

Acknowledgments

Carol Kelly assisted in preparation of this manuscript. The authors thank Dr. David E. Birk for assistance in TEM, and Ms. Noriko Udagawa for genotyping and mouse care. This study was supported by NIAMS/NIH grants R01 AR28450-26, R01 AR52627-7 and R01 AR55225-1. Dr. Jiang is the recipient of a Dermatology Foundation Research Career Development Award.

Abbreviations

PXE	pseudoxanthoma elasticum
KO	knock-out
WT	wild-type

References

Belinsky MG, Kruh GD. MOAT-E (ARA) is a full length MRP/cMOAT subfamily transporter expressed in kidney and liver. Br J Cancer. 1999; 80:1342–1349. [PubMed: 10424734]

Belinsky MG, Chen ZS, Shchaveleva I, Zeng H, Kruh GD. Characterization of the drug resistance and transport properties of multi-drug resistance protein 6 (MRP6, *ABCC6*). Cancer Res. 2002; 62:6172–6177. [PubMed: 12414644]

NIH-PA Author Manuscript

NIH-PA Author Manuscript

NIH-PA Author Manuscript

Capla JM, Ceradini DJ, Tepper OM, Callaghan MJ, Bhatt KA, Galiano RD, et al. Skin graft vascularization involves precisely regulated regression and replacement of endothelial cells through both angiogenesis and vasculogenesis. Plast Reconstr Surg. 2006; 117:836–844. [PubMed: 16525274]

Carson FL. Histotechnology: A Self-Instructional Text. American Society of Clinical Pathology. 1997:222.

Gheduzzi D, Boraldi F, Annovi G, DeVincenzi CP, Schurgers LJ, Vermeer C, Quaglino D, Ronchetti IP. Matrix Gla protein is involved in elastic fiber calcification in the dermis of pseudoxanthoma elasticum patients. Lab Invest. 2007; 87:998–1008. [PubMed: 17724449]

Hendig D, Arndt M, Szliska C, Kleesiek K, Götting C. SPP1 promoter polymorphisms: identification of the first modifier gene for pseudoxanthoma elasticum. Clin Chem. 2007; 53:829–836. [PubMed: 17384004]

Hendig D, Zarbock R, Szliska C, Kleesiek K, Götting C. The local calcification inhibitor matrix Gla protein in pseudoxanthoma elasticum. Clin Biochem. 2008; 41:407–412. [PubMed: 18222176]

Iliás A, Urban Z, Seidl TL, Le Saux O, Sinkó E, Boyd CD, et al. Loss of ATP-dependent transport activity in pseudoxanthoma elasticum-associated mutants of human ABCC6 (MRP6). J Biol Chem. 2002; 277:16860–16867. [PubMed: 11880368]

Jiang Q, Li Q, Uitto J. Aberrant mineralization of connective tissues in a mouse model of pseudoxanthoma elasticum: systemic and local regulatory factors. J Invest Dermatol. 2007; 127:1392–4102. [PubMed: 17273159]

Klement JF, Matsuzaki Y, Jiang Q-J, Terlizzi J, Choi HY, Fujimoto N, et al. Targeted ablation of the ABCC6 gene results in ectopic mineralization of connective tissues. Mol Cell Biol. 2005; 25:8299–8310. [PubMed: 16135817]

LaRusso J, Jiang Q, Li Q, Uitto J. Ectopic mineralization of connective tissue in Abcc6(−/−) mice: effects of dietary modifications and a phosphate binder - a preliminary study. Exp Dermatol. 2007; 17:203–207. [PubMed: 17979973]

LeSaux O, Bunda S, Van Wart CM, Douet V, Got L, Martin L, Hinek A. Serum factors from pseudoxanthoma elasticum patients alter elastic fiber formation in vitro. J Invest Dermatol. 2006; 126:1497–1505. [PubMed: 16543900]

Li Q, Jiang Q, Uitto J. Pseudoxanthoma Elasticum: Oxidative Stress and Antioxidant Diet in a Mouse Model ($Abcc6^{-/-}$). J Invest Dermatol. 2007 (in press).

Li Q, Jiang Q, Pfendner E, Váradi A, Uitto J. Pseudoxanthoma elasticum: clinical phenotypes, molecular genetics and putative pathomechanisms. Exp Derm. 2008 (submitted).

Matsuo S, Kurisaki A, Sugino H, Hashimoto I, Nakanishi H. Analysis of skin graft survival using green fluorescent protein transgenic mice. J Med Invest. 2007; 54:267–275. [PubMed: 17878676]

Matsuzaki Y, Nakano A, Jiang QJ, Pulkkinen L, Uitto J. Tissue-specific expression of the ABCC6 gene. J Invest Dermatol. 2005; 125:900–905. [PubMed: 16297187]

Mombaerts P, Iacomini J, Johnson RS, Herrup K, Tonegawa S, Papaioannou VE. RAG-1-deficient mice have no mature B and T lymphocytes. Cell. 1992; 68:869–877. [PubMed: 1547488]

Neldner, KH.; Struk, B. Pseudoxanthoma elasticum. In: Royce, PM.; Steinmann, B., editors. Connective tissue and its heritable disorders: Molecular, genetic and medical aspects. Wiley-Liss, Inc; NY: 2002. p. 561-583.

Pfendner EG, Vanakker OM, Terry SF, Vourthis S, McAndrew PE, McClain MR, et al. Mutation detection in the *ABCC6* gene and genotype-phenotype analysis in a large international case series affected by pseudoxanthoma elasticum. J Med Genet. 2007; 44:621–628. [PubMed: 17617515]

Pfendner E, Uitto J, Gerard GF, Terry SF. Pseudoxanthoma elasticum: Genetic diagnostic markers. Exp Opinion Med Diagn. 2008; 2:1–17.

Quaglino D, Boraldi F, Barbieri D, Croce A, Tiozzo R, Pasquali-Ronchetti I. Abnormal phenotype of in vitro dermal fibroblasts from patients with pseudoxanthoma elasticum (PXE). Biochim Biophys Acta. 2000; 1501:51–62. [PubMed: 10727849]

Quaglino D, Sartor L, Garbisa S, Boraldi F, Croce A, Passi A, et al. Dermal fibroblasts from pseudoxanthoma elasticum patients have raised MMP-2 degradative potential. Biochim Biophys Acta. 2005; 1741:42–47. [PubMed: 15955448]

NIH-PA Author Manuscript

NIH-PA Author Manuscript

NIH-PA Author Manuscript

Ringpfeil F, Pulkkinen L, Uitto J. Molecular genetics of pseudoxanthoma elasticum. Exp Dermatol. 2001; 10:221–228. [PubMed: 11493310]

Scheffer GL, Hu X, Pijnenborg AC, Wijnholds J, Bergen AA, Scheper RJ. MRP6 (*ABCC6*) detection in normal human tissues and tumors. Lab Invest. 2002; 82:515–518. [PubMed: 11950908]

Uitto J, Pulkkinen L, Ringpfeil F. Molecular genetics of pseudoxanthoma elasticum: a metabolic disorder at the environment-genome interface? Trends Mol Med. 2001; 7:13–17. [PubMed: 11427982]

Zarbock R, Hendig D, Szliska C, Kleesiek K, Götting C. Pseudoxanthoma elasticum: genetic variations in antioxidant genes are risk factors for early disease onset. Clin Chem. 2007; 53:1734–1740. [PubMed: 17693525]

NIH-PA Author Manuscript

NIH-PA Author Manuscript

NIH-PA Author Manuscript

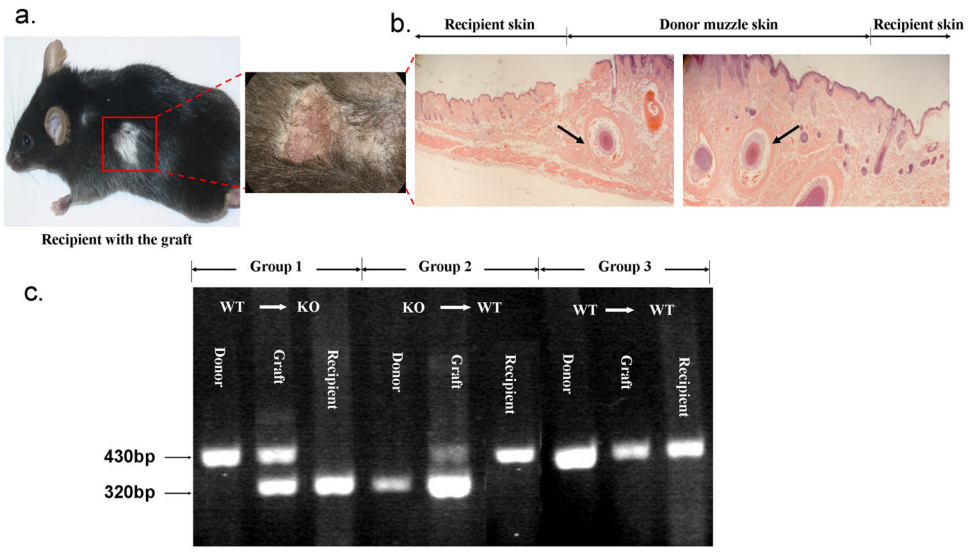

Figure 1. Grafting of muzzle skin to the back of mice

Hair on the back of the recipient mice was clipped and a full thickness skin wound bed (0.5–1.0 cm in diameter) was prepared. The similar size sample of muzzle skin was obtained from the donor mice and grafted into the wound bed on the back of the recipient mice. The grafts were examined at 2 months after surgery by morphologic observations (a), by histology using H&E staining (b), and by genomic PCR (c). In (b), the arrows point to cross-sections of vibrissae in the graft of the donor mouse muzzle skin while they are not present in the adjacent back skin of the recipient mouse. In (c), the 430-bp band represents the wild-type allele, while the 320-bp PCR product is derived from amplification of knock-out (*Abcc6*$^{-/-}$) allele.

NIH-PA Author Manuscript

NIH-PA Author Manuscript

NIH-PA Author Manuscript

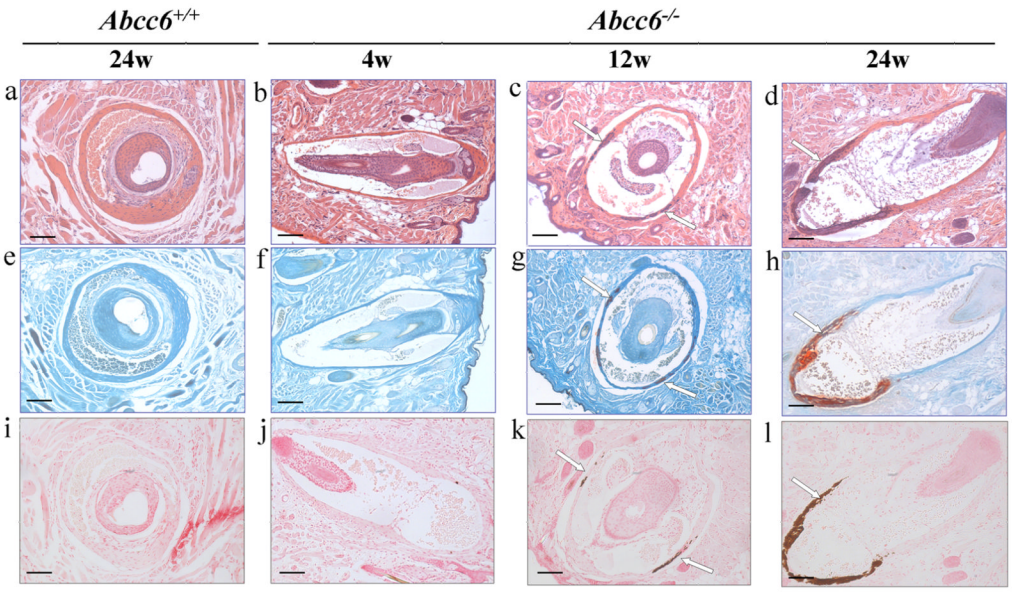

Figure 2. Progressive mineralization of connective tissue capsule of vibrissae in *Abcc6*$^{-/-}$ mice with age

Sections of muzzle skin from 24-week old *Abcc6*$^{+/+}$ mice as well as from *Abcc6*$^{-/-}$ mice at 4, 12 and 24 weeks of age were stained with H&E (top panel), Alizarin Red (middle panel) or von Kossa (bottom panel). No mineralization was noted in the 24-week old *Abcc6*$^{+/+}$ mice (a,e and i), nor was there any mineralization in the 4-week old *Abcc6*$^{-/-}$ mice (b,f and j). In contrast, mineralization, as reflected by dark purple (top, c and d, arrows), red color (middle, g and h, arrows) or dark brown (bottom, k and l, arrows), was noted in the 12-week and 24-week old *Abcc6*$^{-/-}$ mice which demonstrated a progressive increase in mineralization with advancing age. Scale bar = 100 μm

NIH-PA Author Manuscript
NIH-PA Author Manuscript
NIH-PA Author Manuscript

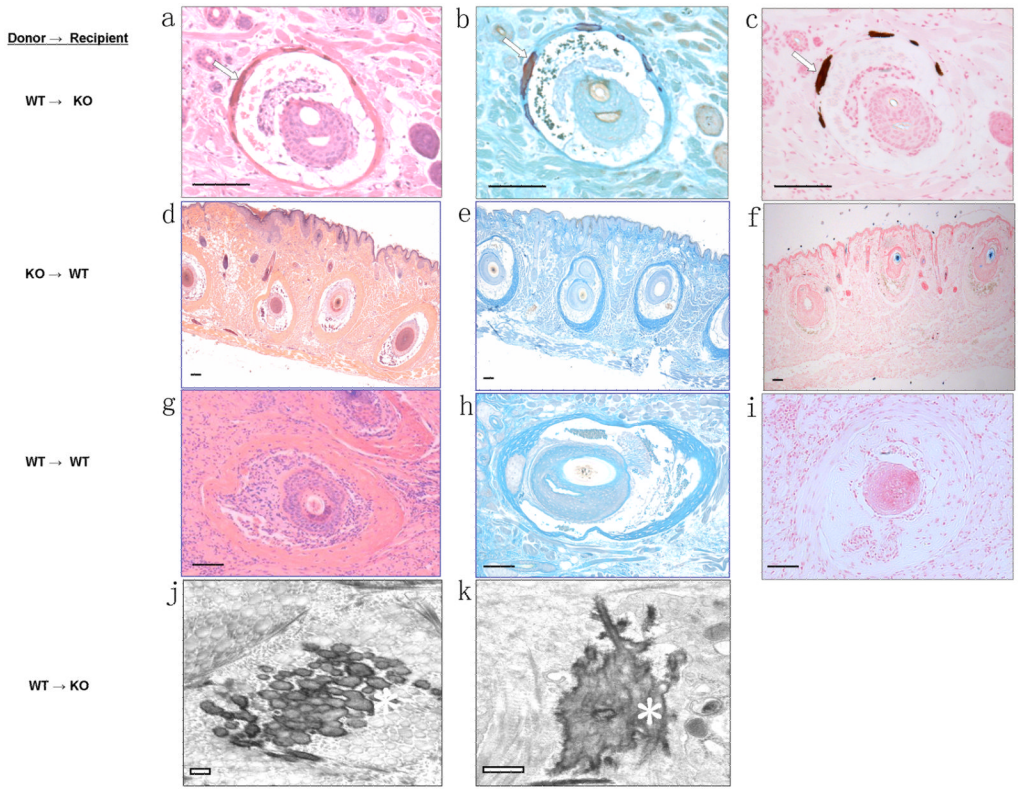

Figure 3. Aberrant mineralization of the connective tissue capsule of vibrissae in grafted skin

Two months after transplantation of grafts from 4-week old donor mice onto the back of recipient mice, the grafts were harvested and the mineralization was examined by H&E (a, d and g), Alizarin Red (b, e and h) and von Kossa (c, f and i) stains and by transmission electron microscopy (j, k). The connective tissue capsule of vibrissae grafted from the muzzle skin of *Abcc6*$^{+/+}$ mice onto the back of *Abcc6*$^{-/-}$ mice developed characteristic mineralization (a–c, arrows), while no mineralization was observed in the grafts either from *Abcc6*$^{-/-}$ (d–f) or *Abcc6*$^{+/+}$ (g–i) mice when transplanted onto the back of WT mice. TEM revealed mineralization (asterisks) of both collagen fibers (j) and elastic structures (k) in the vibrissae of *Abcc6*$^{+/+}$ mice at 2 months after grafting onto *Abcc6*$^{-/-}$ mice. Scale bar = 100 μm (a–i); 1 μm (j and k).

NIH-PA Author Manuscript
NIH-PA Author Manuscript
NIH-PA Author Manuscript

TABLE 1

Mineralization of Vibrissae in Grafted Skin[a]

	Group[b] (Donor → Recipient)	Total Vibrissae[c] (n)	Mineralized vibrissae[c] (n)	Percent mineralized (%)
1.	WT → KO (n=8)	56	16	28.6
2.	KO → WT (n=7)	42	0	0
3.	WT → WT (n=4)	12	0	0

[a]Tissue samples of muzzle skin from the donor mice were grafted on the wound bed on the back of recipient mice at four weeks of age, as shown in Fig. 1. The grafts were analyzed for mineralization two months post-grafting by staining with H&E and Alizarin Red, as shown in Fig. 3a.

[b]KO, knockout (Abcc6−/−) mice; WT, wild-type mice.

[c]n, numbers of vibrissae examined

J Invest Dermatol. Author manuscript; available in PMC 2011 September 8.

NIH-PA Author Manuscript NIH-PA Author Manuscript NIH-PA Author Manuscript

TABLE 2

Quantitation of Mineralization of Vibrissae 3 Months after Being Grafted[a]

Experimental Group[b] (Donor → Recipient)	Total vib. per graft[c] (n)	Mineralized vib. per graft[c] (n)	Percent mineralized (%)	Total area per graft[d] (U × 10^3)	Mineralized area per graft[d] (U × 10^3)	Area of mineralization per total area[e] (%)	Fold[f]	P value
KO → WT (6m, n=6)	20.17	3.33	21.1	18.597	0.134	0.52 ± 0.24 (0.34; 0–1.28)	0.16	<0.01[g] >0.05[h]
KO → KO (6m, n=4)	14.25	6.75	47.9	32.366	0.921	3.19 ± 1.28 (2.32; 1.17–6.94)	1.0	
KO (3m, n=11)	10.00	5.64	59.2	82.258	0.996	1.21 ± 0.19 (1.20; 0.37–2.40)	0.40	<0.05[i]

[a] Skin sections from KO mice at the age of 3 months (m) were grafted onto the back of either WT or KO mice. Three months post-grafting, the grafts were removed, stained with H&E, and examined for mineralization by light microscopy followed by quantitative computerized morphometric analysis. For comparison, KO mice at 3m of age were examined similarly for mineralization.

[b] WT, wild-type (*Abcc6*$^{+/+}$); KO, knockout (*Abcc6*$^{-/-}$) mice.

[c] n, numbers of vibrissae examined.

[d] Units are expressed as pixels per μm^2 reflecting the intensity of H&E stain.

[e] Values presented as mean + S.E.M. as well as median; range in parenthesis.

[f] Calculated using the KO →KO group as 1.0.

[g] p-value for comparison between KO → WT and KO → KO groups (one-way ANOVA followed by Bonferroni's multiple comparison test).

[h] p-value for comparison between KO → WT and KO groups (one-way ANOVA followed by Bonferroni's multiple comparison test).

[i] p-value for comparison between KO → KO and KO groups (one-way ANOVA followed by Bonferroni's multiple comparison test).